$$\Delta G^{\circ\prime} = 2.3RT[pK_a^A - pK_a^B] \quad (41)$$

The combination of eq 40 and 41 with the Marcus eq 26 yields

$$\log \kappa = A + B[pK_a^B] + C[pK_a^B]^2 \quad (42)$$

where $A = -(RT \ln 10)^{-1}\{w^r + \Delta G^{\ddagger}_0 + [pK_a^A](RT \ln 10)/2 + [pK_a^A]^2(RT \ln 10)^2/16\Delta G^{\ddagger}_0\} + \ln Z/n + \mathcal{F}\Delta E/RT$, $B = (RT \ln 10)^{-1}[pK_a^A]/8\Delta G^{\ddagger}_0 + {}^1/_2$, and $C = -(RT \ln 10)/16\Delta G^{\ddagger}_0$. The solution of eq 42 was carried out by a polynomial regression analysis on a Digital Equipment Corp. 11/23 computer using a MINC basic subroutine in which log κ was the dependent variable and $[pK_a^B]$ the independent variable. The second-order coefficient $C = -0.013154$ yielded the values of $\Delta G^{\ddagger}_0$, the first-order coefficient $B = 0.551694$ yielded the value of $[pK_a^A]$, and the zero-order term $A = -7.35117$ yielded the value of w^r with a correlation coefficient of 0.995 for all the data in Table V excluding 2,6-di-*tert*-butylpyridine (see text).

Acknowledgment. We thank J. Goncalves for the computer program for multiple regression analysis of the kinetics data, the National Science Foundation for financial support, and the United States-France (NSF-CNRS) cooperative program for the award of a fellowship to C.A.

Registry No. $Fe(phen)_3(PF_6)_3$, 28277-57-8; Dz, 7782-39-0; hexamethylbenzene, 87-85-4; pentamethylbenzene, 700-12-9; 1,2,4,5-tetramethylbenzene, 95-93-2; 1,2,3,4-tetramethylbenzene, 488-23-3; 1,2,3,5-tetramethylbenzene, 527-53-7; hexamethylbenzene cation radical, 34473-51-3; 1,2,4,5-tetramethylbenzene cation radical, 34473-49-9; pentamethylbenzene cation radical, 34473-50-2; 1,2,3,4-tetramethylbenzene cation radical, 34528-28-4; 2-fluoropyridine, 372-48-5; 2-chloropyridine, 109-09-1; 3-pyridinecarbonitrile, 100-54-9; 4-pyridinecarbonitrile, 100-48-1; 3-chloropyridine, 626-60-8; 3-fluoropyridine, 372-47-4; pyridine, 110-86-1.

Reaction Mechanisms of Oxidative Addition [$H_2 + Pt^0(PH_3)_2 \rightarrow Pt^{II}(H)_2(PH_3)_2$] and Reductive Elimination [$Pt^{II}(H)(CH_3)(PH_3)_2 \rightarrow CH_4 + Pt^0(PH_3)_2$]. Ab Initio MO Study

Shigeru Obara,[1a,b] Kazuo Kitaura,[1a,c] and Keiji Morokuma*[1a]

Contribution from the Institute for Molecular Science, Myodaiji, Okazaki 444, Japan, and the Department of Chemistry, Kyoto University, Kyoto 606, Japan. *Received March 5, 1984*

Abstract: Reaction mechanisms of the oxidative addition of H_2 to two-coordinate $Pt^0(PH_3)_2$ and the reductive elimination of CH_4 from four-coordinate $Pt^{II}(H)(CH_3)(PH_3)_2$ are studied by ab initio RHF and CI calculations with the energy gradient method within the framework of the relativistic effective core potential approximation for Pt core electrons. Fully optimized geometries of transition states of both reactions as well as the reactants and products have been obtained. The fact that the oxidative addition more commonly takes place for H_2 and only the reductive elimination does for CH_4 can be explained in terms of calculated exothermicity. The H_2 oxidative-addition reaction is suggested to pass through an early transition state that would lead directly to a cis product and then to be pushed toward a trans product by a steric repulsion between bulky phosphine ligands. A large deuterium kinetic isotope effect experimentally found in the reductive elimination reaction of CH_3D from $Pt(D)(CH_3)(PPh_3)_2$ is accounted for in terms of the calculated four-coordinate transition state, where the reaction coordinate is CPtH bending. A decrease in the interligand angle has been found to increase the reactivity of the metal center by selectively activating one of the d orbitals. Both donation and back-donation between the metal and H_2 have been found to be important at the transition state of the H_2 addition reaction.

The oxidative addition of molecular hydrogen and aliphatic RH and the corresponding reverse reductive elimination are important reactions as elementary processes in many catalytic and synthetic reactions.[2] Recent studies by Otsuka, Yoshida, and their colleagues on preparation and reaction of H_2 with two-coordinate platinum(0) [and palladium(0)] phosphine complexes present an interesting chemistry of homogeneous catalytic activities.[3-5] Some of them easily absorb molecular hydrogen[4] at room temperature to give dihydride complexes, which are identified by NMR and IR studies to be trans products. Oxidative-addition products have been found to be diamagnetic, indicating a closed-shell singlet ground state, which is reasonable for d^8 square-planar complexes.[6] Reversible reactions with H_2 at room temperature[5] are also found for some of Pt(0)-chelating phosphine complexes. The symmetry rule suggests that the oxidative addition of H_2 occurs in a cis fashion;[2] however, a trans mechanism has been proposed for the addition of H_2 to Ir complexes.[7]

The reductive-elimination reaction of CH_4 from $Pt(H)(CH_3)(PPh_3)_2$ has been found by Abis, Sen, and Halpern.[8] The reaction rate was unaffected by the presence of excess phosphine ligands, suggesting strongly that the elimination proceeds through a four-coordinate transition state. They observed a large deuterium kinetic isotope ratio of 3.3 for the decomposition reaction of $Pt(D)(CH_3)(PPh_3)_2$. On the other hand, small isotope ratios of 1.2-1.3 have been observed for H_2 and RH oxidative-addition reactions.[9,10] The oxidative addition of aliphatic CH is considered to occur in a H-D exchange reaction of alkane with K_2PtCl_4[11] as a catalyst and in an internal metalation[12] where a CH bond in a ligand such as PR_3 is broken, although in both of the reactions the RH adduct has not been isolated. However, aromatic and olefinic CH's are known to add oxidatively to Ir, Pd, Fe, Ru, and Os compounds.[13]

(1) (a) Institute for Molecular Science. (b) Kyoto University. (c) Present address: Department of Chemistry, Osaka City University, Osaka 558, Japan.
(2) (a) Collman, J. P. *Acc. Chem. Res.* **1968**, *1*, 136. (b) Halpern, J. *Acc. Chem. Res.* **1970**, *3*, 386. (c) Vaska, L.; Werneke, M. F. *Trans. N. Y. Acad. Sci.* **1971**, *33*, 70. (d) Longato, B.; Morandini, F.; Bresadola, S. *Inorg. Chem.* **1976**, *15*, 650.
(3) Otsuka, S.; Yoshida, T.; Matsumoto, M.; Nakatsu, K. *J. Am. Chem. Soc.* **1976**, *98*, 5850.
(4) Yoshida, T.; Otsuka, S. *J. Am. Chem. Soc.* **1977**, *99*, 2134.
(5) Yoshida, T.; Yamagata, T.; Tulip, T. H.; Ibers, J. A.; Otsuka, S. *J. Am. Chem. Soc.* **1978**, *100*, 2063.
(6) Hartley, F. R. "The Chemistry of Platinum and Palladium"; Applied Science Publishers: London, 1973; Appendix II.
(7) Harrod, J. F.; Hamer, G.; Yorke, W. *J. Am. Chem. Soc.* **1979**, *101*, 3987.
(8) Abis, L.; Sen, A.; Halpern, J. *J. Am. Chem. Soc.* **1978**, *100*, 2915.
(9) Chock, P. B.; Halpern, J. *J. Am. Chem. Soc.* **1966**, *88*, 3511.
(10) Brown, J. M.; Parker, D. *Organometallics* **1982**, *1*, 950.
(11) Webster, D. E. *Adv. Organomet. Chem.* **1979**, *15*, 147.
(12) Goel, R. G.; Montemayor, R. G. *Inorg. Chem.* **1977**, *16*, 2183.

0002-7863/84/1506-7482$01.50/0

Many reductive-elimination reactions of RR′ have been found for Ni, Pd, and Pt compounds.[14] The oxidative addition of RR′, however, has not been found, except for metallacycle formation with strained ring hydrocarbons such as a reaction of cubane with a rhodium compound[15] and a reaction of cyclopropane with a platinum compound.[16]

From a study of $Pd[PPh(t\text{-}Bu)_2]_2$ and $Pt[PPh(t\text{-}Bu)_2]_2$, where O_2 coordination is reversible for the former while it is irreversible for the latter, Otsuka et al. have suggested the difference in an interligand angle as an origin of this reactivity difference and proposed to control the reactivity of metal phosphine complexes with the interligand angle as well as the steric size and basicity of phosphine ligands.[17,18]

A few theoretical studies have been published on these reactions. Hoffmann et al. studied the reductive elimination of alkane from dialkyl Ni, Pd, Pt, and Au compounds by the extended Hückel method.[19] The oxidative addition of H_2 to $RhCl(PH_3)_3$ has been studied by Dedieu and Strich with the extended Hückel[20] and the ab initio method.[21] They examined possible schemes of hydrogenation of olefins catalyzed by rhodium compounds.[21] The bonding interaction between the H_2 antibonding orbital and an occupied Rh d orbital has been suggested to facilitate HH bond breaking in this reaction as well as in the $(C_5H_5)_2Mo + H_2$ reaction.[22] Whitesides et al.[23] discussed a correlation between the relative rates of reductive elimination ($L_2MXY \rightarrow L_2M + XY$; L = PH_3; M = Pt, Pd, and Ni; XY = $(H)_2$, $(H)(CH_3)$, and $(CH_3)_2$) and the molecular orbital character of the starting compounds using self-consistent field–Xα–scattered-wave calculations.

Noell and Hay have recently studied the oxidative-addition reactions $H_2 + Pt(PH_3)_2 \rightarrow$ *cis*-$Pt(H)_2(PH_3)_2$ and $H_2 + Pt([P(CH_3)_3]_2 \rightarrow$ *cis*-$Pt(H)_2[P(CH_3)_3]_2$ by ab initio HF, MCSCF, and CI methods with a relativistic effective core potential and a flexible Gaussian basis set for the valence electrons.[24] They optimized three important geometrical parameters within C_{2v} symmetry by the energy method and determined relative energies of reactants, products, and transition states. They obtained an exothermicity of 7 kcal/mol and an activation barrier of 17 kcal/mol and therefore a barrier of 24 kcal/mol for the reverse reductive elimination.

Scheme I

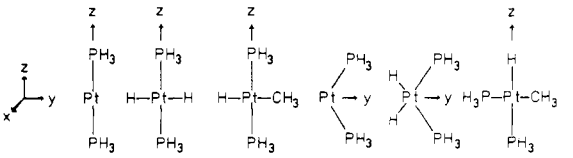

Recently the energy gradient method in the ab initio MO method has become a most powerful tool for exploring potential energy surfaces.[25] In the method the first derivative, i.e., the gradient of the electronic energy with respect to nuclear coordinates is evaluated analytically and efficiently. The gradient is then used to locate the equilibrium and the transition-state geometry in which all the geometrical parameters are fully optimized. The force constant matrix is evaluated by numerical differentiation of the gradient. The energy gradient method has been applied in the ab initio MO method to many reaction systems with several first-row atoms and their transition states have been determined.[25] However until recently[26-28] the gradient method has not been used for transition-metal reactions. We have published preliminary results of fully optimized molecular structures of two-coordinate Pt(0) diphosphine, $Pt(PH_3)_2$, four-coordinate *cis*- and *trans*-$Pt(H)_2(PH_3)_2$,[26] and a transition state of oxidative addition of H_2 to $Pt(PH_3)_2$.[27]

In this paper we report a full account of our ab initio MO study of the oxidative addition reaction of H_2 to $Pt(PH_3)_2$ as well as the reductive elimination of CH_4 from $Pt(H)(CH_3)(PH_3)_2$. The purposes of the study are as follows: (1) to check how well the present method reproduces equilibrium geometries and IR normal mode frequencies by comparing them with the experimental results, (2) to elucidate features of potential surfaces for reactions of H_2 and CH_4 with Pt(0) diphosphines by determining transition-state geometries and energies and to compare differences between H_2 reactions and CH_4 reactions, (3) to calculate theoretical values of the deuterium kinetic isotope ratio for the reductive elimination of $Pt(D)(CH_3)(PH_3)_2$ and the oxidative addition of D_2 to $Pt(PH_3)_2$, to be compared with experiments, (4) to investigate, using a theoretical model, the effect of the interligand PPtP angle on the reactivity, and (5) to discuss detailed mechanisms of oxidative-addition and reductive-elimination reactions. The second section describes methods of calculation. Results and discussions are given in the third and fourth sections, followed by a summary in the last section.

Methods of Calculation

We have optimized all the geometrical parameters of $Pt(PH_3)_2$, cis and trans forms of $Pt(H)_2(PH_3)_2$ and $Pt(H)(CH_3)(PH_3)_2$, and the transition states (Scheme I) by using the energy gradient technique[26] at the restricted Hartree–Fock (RHF) level under the effective core potential (ECP) approximation.[29] Calculations were performed for a closed-shell singlet state, the ground state. A smaller basis set was used in geometry optimization and normal mode calculations. This basis set consists of valence double (3s3p5d)/[2s2p2d] set[29] for Pt, 3-21G[30] for the hydride H and the methyl group, and STO-2G[31] for PH_3. The relativistic ECP obtained by Basch and Topiol[29] was used to replace core electrons for Pt. The smaller basis set reproduces well the geometries of

(13) (a) Abicht, H. P.; Issleib, K. *Z. Chem.* **1977**, *17*, 1. (b) Guss, J. M.; Mason, R. *J. Chem. Soc., Chem. Commun.* **1971**, 58. (c) Hietkamp, S.; Stufkens, D. J.; Vrieze, K. *J. Organomet. Chem.* **1977**, *139*, 189. (d) Tolman, C. A.; Ittel, S. D.; English, A. D.; Jesson, J. P. *J. Am. Chem. Soc.* **1979**, *101*, 1742. (e) Komiya, S.; Ito, T.; Cowie, M.; Yamamoto, A.; Ibers, J. A. *J. Am. Chem. Soc.* **1976**, *98*, 3874. (f) Kubota, M.; Miyashita, A.; Komiya, S.; Yamamoto, A. *J. Organomet. Chem.* **1977**, *139*, 111. (g) Deeming, A.; Underhill, M. *J. Chem. Soc., Chem. Commun.* **1973**, 277.

(14) (a) Gillie, A.; Stille, J. K. *J. Am. Chem. Soc.* **1980**, *102*, 4933. (b) Ozawa, F.; Ito, T.; Nakamura, Y.; Yamamoto, A. *Bull. Chem. Soc. Jpn.* **1981**, *54*, 1868. (c) Tatsumi, K.; Hoffmann, R.; Yamamoto, A.; Stille, J. K. *Bull. Chem. Soc. Jpn.* **1981**, *54*, 1857. (d) Brown, M. P.; Puddephatt, R. J.; Upton, C. E. E. *J. Chem. Soc., Dalton Trans.* **1974**, 2457. (e) Doyle, M. J.; McMeeking, J.; Binger, P. *J. Chem. Soc., Chem. Commun.* **1976**, 376. (f) Binger, P.; Doyle, J. H.; Kruger, C.; Tsay, Y. H. *Z. Naturforsch., B: Anorg. Chem., Org. Chem.* **1979**, *34B*, 1289. (g) DiCosimo, R.; Whitesides, G. M. *J. Am. Chem. Soc.* **1982**, *104*, 3601.

(15) (a) Halpern, J. "Organic Synthesis via Metal Carbonyls"; Wender, P. Pino, Ed.; Wiley: New York 1977; Vol. I, II. (b) Bishop, K. C. *Chem. Rev.* **1976**, *76*, 461. (c) Cassar, L.; Eaton, P. E.; Halpern, J. *J. Am. Chem. Soc.* **1970**, *92*, 3515.

(16) (a) Puddephatt, R. J.; Quyser, M. A.; Tipper, C. F. H. *J. Chem. Soc., Chem. Commun.* **1976**, 626. (b) Puddephatt, R. J. *Coord. Chem. Rev.* **1980**, *33*, 149. (c) Klingler, R. J.; Hoffmann, J. C.; Kochi, J. K. *J. Am. Chem. Soc.* **1982**, *104*, 2147. (d) Rajaram, J.; Ibers, J. A. *J. Am. Chem. Soc.* **1978**, *100*, 829. (e) Graziani, M.; Lenarda, M.; Ros, R.; Belluco, U. *Coord. Chem. Rev.* **1975**, *16*, 35. (f) Yarrow, D. J.; Ibsers, J. A.; Lenarda, M.; Graziani, M. *J. Organomet. Chem.* **1974**, *70*, 133.

(17) Yoshida, T.; Tatsumi, K.; Matsumoto, M.; Nakatsu, K.; Nakamura, A.; Fueno, T.; Otsuka, S. *Nouv. J. Chim.* **1979**, *3*, 761.

(18) Yoshida, T.; Tatsumi, K.; Otsuka, S. *Pure Appl. Chem.* **1980**, *52*, 713.

(19) Tatsumi, K.; Hoffmann, R.; Yamamoto, A.; Stille, J. K. *Bull. Chem. Soc. Jpn.* **1981**, *54*, 1857.

(20) Dedieu, A.; Strich, A. *Inorg. Chem.* **1979**, *18*, 2940.

(21) Dedieu, A. *Inorg. Chem.* **1980**, *19*, 375.

(22) Lauher, J. W.; Hoffmann, R. *J. Am. Chem. Soc.* **1976**, *98*, 1729.

(23) Balazs, A. C.; Johnson, K. H.; Whitesides, G. M. *Inorg. Chem.* **1982**, *21*, 2162.

(24) (a) Noell, J. O.; Hay, P. J. *J. Am. Chem. Soc.* **1982**, *104*, 4578. (b) Noell, J. O.; Hay, P. J. *Inorg. Chem.* **1982**, *21*, 14.

(25) Morokuma, K.; Kato, S.; Kitaura, K.; Obara, S.; Ohta, K.; Hanamura, M. "New Horizons of Quantum Chemistry"; Lowdin, P.-O., Pullman, B., Eds.; D. Reidel Publishing: Dordrecht, Netherlands, 1983; p 221.

(26) Kitaura, K.; Obara, S.; Morokuma, K. *Chem. Phys. Lett.* **1981**, *77*, 452.

(27) Kitaura, K.; Obara, S.; Morokuma, K. *J. Am. Chem. Soc.* **1981**, *103*, 2891.

(28) Sakaki, S.; Kitaura, K.; Morokuma, K.; Ohkubo, K. *J. Am. Chem. Soc.* **1983**, *105*, 2280.

(29) Basch, H.; Topiol, S. *J. Chem. Phys.* **1979**, *71*, 802.

(30) Binkley, J. S.; Pople, J. A.; Hehre, W. J. *J. Am. Chem. Soc.* **1980**, *102*, 939.

(31) Hehre, W. J.; Stewart, R. F.; Pople, J. A. *J. Chem. Phys.* **1969**, *51*, 2657.

Table I. Mulliken Population Analysis of $Pt(PH_3)_2$, $Pt(H)_2(PH_3)_2$, and $Pt(H)(CH_3)(PH_3)_2$[a]

	linear $Pt(PH_3)_2$	*trans*-$Pt(H)_2$-$(PH_3)_2$	*trans*-Pt(H)-$(CH_3)(PH_3)_2$	bent $Pt(PH_3)_2$[b]	*cis*-$Pt(H)_2$-$(PH_3)_2$	*cis*-Pt(H)-$(CH_3)(PH_3)_2$	transition state $Pt(H)_2$-$(PH_3)_2$[c]	transition state Pt(H)-$(CH_3)(PH_3)_2$[d]	CH_4
					Gross[e]				
Pt	10.52	10.67	10.39	10.23	10.67	10.43	10.40	10.39	
s	0.96	0.81	0.73	0.43	0.91	0.83	0.62	0.59	
p	0.18	0.89	0.74	0.36	0.76	0.67	0.41	0.56	
x	0.01	0.01	0.03	0.02	0.02	0.04	0.01	0.02	
y	0.02	0.67	0.48	0.07	0.39	0.27	0.17	0.26	
z	0.15	0.21	0.23	0.28	0.35	0.36	0.23	0.28	
d	9.38	8.98	8.92	9.43	9.00	8.93	9.37	9.24	
xy	2.00	2.00	1.99	1.94	1.96	1.93	1.99	1.91	
xz	1.88	1.92	1.92	1.90	1.93	1.94	1.89	1.96	
yz	1.88	1.93	1.93	1.87	1.33	1.90	1.82	1.73	
x^2	1.43	1.42	1.43	1.49	1.42	1.43	1.46	1.46	
y^2	1.43	0.92	0.87	1.15	1.20	0.83	1.30	1.06	
z^2	0.77	0.78	0.78	1.08	1.17	0.90	0.90	1.11	
H		1.03	1.02		0.95	0.97	0.97	0.76	0.80
PH_3	7.74	7.63	7.64	7.88	7.71	7.68	7.83	7.82, 7.87[f]	
CH_3			9.31			9.24		9.16	9.20
					Overlap				
Pt–H		0.38	0.38		0.39	0.39		0.18	
Pt–P	0.35	0.33	0.33	0.31	0.26	0.25		0.34, 0.28[f]	
Pt–C			0.29		0.32			0.13	

[a] The analysis is based on RHF calculation with the larger basis set. The direction of the coordinate axes is shown in Scheme I. [b] The molecular geometry of the bent $Pt(PH_3)_2$ is set to be the same as that of the corresponding *cis*-$Pt(H)_2(PH_3)_2$. [c] The Pt and two P atoms are on the *yz* plane, and the symmetry axis is on the *y* axis. [d] The Pt and two P atoms are on the *yz* plane, and the PtH bond is on the *z* axis. [e] Core electrons of Pt and P atoms are not taken into account. Therefore the total gross populations of a free Pt atom and PH_3 molecule become 10 and 8, respectively. [f] The former value corresponds to the PH_3 adjacent to the hydride.

$Pt(PH_3)_2$, *cis*-$Pt(H)_2(PH_3)_2$, and *trans*-$Pt(H)_2(PH_3)_2$ obtained by the larger basis set.[26] The larger set is obtained from the smaller set by replacing basis functions for H by 21G and P by LP-31G with the nonrelativistic ECP approximation.[32] In calculations of relative energies of reactants, products, and transition states, configuration interaction calculations including all the single and double excitations of valence electrons relative to the RHF configuration,[33] often called SD-CI, were carried out with the larger basis set at the geometries optimized at the smaller basis RHF level. The number of configurations included amounts to be about 67 000 and 150 000 for $Pt(H)_2(PH_3)_2$ and $Pt(H)(CH_3)(PH_3)_2$, respectively, in the C_s symmetry. The correction for unlinked quadruple excitations, called QC, has also been included on the basis of Davidson's formula.[34]

We used IMSPAK[35] for ECP geometry optimization and the direct CI program in ALCHEMY for CI calculation. For d functions $x^2 + y^2 + z^2$ components are excluded from RHF and CI calculations. Errors caused by the ECP approximation had been examined for geometries and relative energies of the first- and second-row polyatomic molecules.[36]

$Pt(PH_3)_2$, *cis*-$Pt(H)(R)(PH_3)_2$, and *trans*-$Pt(H)(R)(PH_3)_2$ (R = H or CH_3). (A) Electronic Structures. The calculated orbital energy levels of $Pt(PH_3)_2$, *trans*-$Pt(H)_2(PH_3)_2$, and cis-$Pt(H)_2$-$(PH_3)_2$ are given in Figure 1, along with schematic illustrations of orbitals. All the valence occupied orbitals are shown in the figure, except for PH bonding orbitals which lie in the region of −0.6 to −0.5 hartree.

In the linear $Pt(PH_3)_2$ complex d orbital levels are split into three groups, two of which are degenerate as shown in Figure 1.

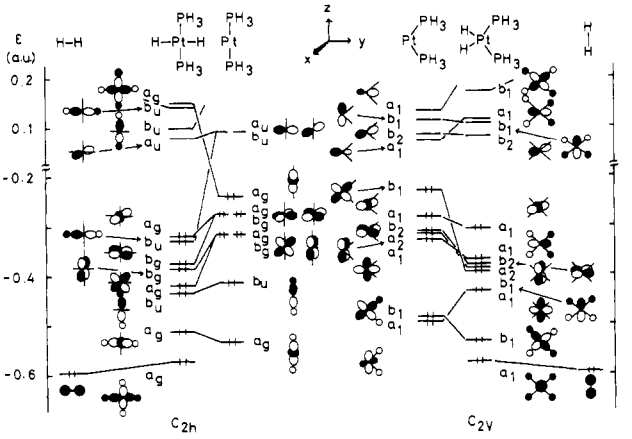

Figure 1. MO levels of *trans*- and *cis*-$Pt(H)_2(PH_3)_2$ as well as those of their $Pt(PH_3)_2$ moieties. The MO symmetry is that of C_{2h} in the left-hand side and that of C_{2v} in the right-hand side.

The highest occupied molecular orbital (HOMO) is mainly the d_{z^2} orbital of the Pt atom, as anticipated from the ligand field theoretical consideration. The degenerate lowest unoccupied molecular orbital (LUMO) consists mainly of Pt p_x and p_y orbitals. Two PtP bonding orbitals lie below d orbital levels, around −0.4 to −0.6 hartree. One of them consists of Pt s and d_{z^2} orbitals and PH_3 lone-pair orbitals. The other is made of the Pt p_z orbital and PH_3 lone pairs. These bonding features in the linear $Pt(PH_3)_2$ complex are recognized also in the Mulliken population, as given in the first column of Table I. Gross populations of 0.96 in s valence orbitals and of 0.18 in p valence orbitals of Pt are evidence of participation into the PtP bond formation by these orbitals, whose gross populations are zero in a free d^{10} singlet Pt atom. The sum of d orbital gross populations is 9.38, though the two-coordinate $Pt(PH_3)_2$ complex is formally called a d^{10} complex.

In forming the *trans*-$Pt(H)_2(PH_3)_2$ complex two hydrogen atoms interact with these MO's to give two bonding orbitals as shown in Figure 1. One is an in-phase mix of the symmetric hydride orbital with Pt $d_{y^2-z^2}$ orbital, and the other consists of the originally vacant Pt p_y orbital and antisymmetric hydride orbitals. The highest occupied a_g orbital in $Pt(PH_3)_2$ becomes unoccupied

(32) From GAUSSIAN 80 (Binkley, J. S.; Whiteside, R. A.; Krishman, R.; Seger, R.; DeFrees, D. J.; Schlegel, H. B.; Topiol, S.; Kahn, L. R.; Pople, J. A.).

(33) Roos, B. D.; Siegbahn, P. In "Method of Electronic Structure Theory"; Schaefer, H. F., Ed.; Plenum Press: New York, 1977; Chapter 7. We used the direct CI program in the ALCHEMY system (Yoshimine, M.; McLean, A. D.; Liu, B.; Dupuis, M.; Bagus, P. S. *Nat. Resour. Comput. Chem. Software Cat.* **1980**, *1*, No. QC03) with a modification to make use of IMSPACK integral files.

(34) Davidson, E. R.; Silver, E. W. *Chem. Phys. Lett.* **1977**, *52*, 403.

(35) Morokuma, K.; Kato, S.; Kitaura, K.; Ohmine, I.; Sakai, S.; Obara, S., IMS Computer Center Library Program, 1980, No. 0372.

(36) Obara, S.; Kitaura, K.; Morokuma, K. *Theor. Chim. Acta* **1981**, *60*, 227.

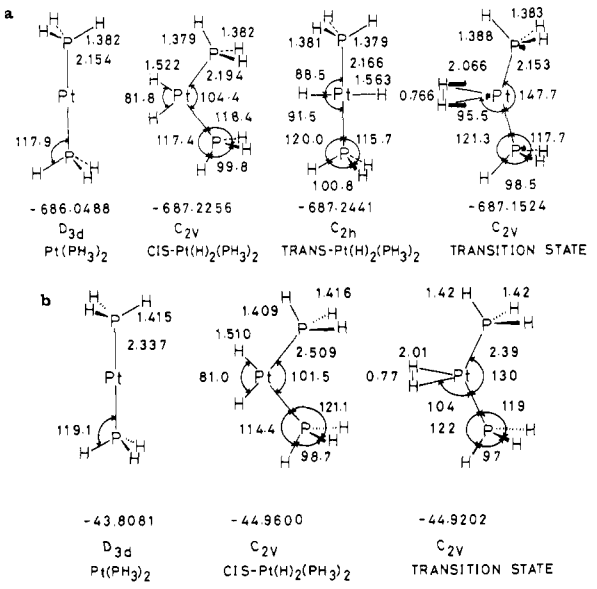

Figure 2. (a) Fully optimized geometries (in Å and deg) of $Pt(PH_3)_2$, *cis*-$Pt(H)_2(PH_3)_2$, *trans*-$Pt(H)_2(PH_3)_2$, and the transition state with their total energies in the smaller basis set. Arrows in the transition state show the reaction coordinate vectors. (b) Fully optimized geometries (in Å and deg) of $Pt(PH_3)_2$, *cis*-$Pt(H)_2(PH_3)_2$, and the transition state (TS) with their total energies by using Noell and Hay's basis set and ECP.[24b] The geometry of TS is converged only up to a few thousands of a angstrom, with the energy error of a few tenths of a mircohartree.

in the trans compound and the lowest unoccupied b_u orbital becomes occupied as shown in the figure. This switching between an occupied and a vacant orbital suggests that the trans addition of H_2 is symmetry forbidden.[37] The bonding scheme in *trans*-$Pt(H)_2(PH_3)_2$ also can be seen from orbital populations given in Table I. A prominent increase of population in the Pt p_y orbital and a remarkable decrease in Pt y^2 and z^2 Cartesian d orbitals show the bonding nature described above.

In a bent $Pt(PH_3)_2$ whose geometry is set to be the same as that of *cis*-$Pt(H)_2(PH_3)_2$, the d levels change their energies from those of the linear structure (right-hand side of Figure 1). The important change is in HOMO; the d_{yz} orbital becomes the highest occupied. LUMO becomes the hybridized Pt s–p_y orbital, directed to the opposite side of PH_3 ligands. When two hydrogen atoms are complexed to form *cis*-$Pt(H)_2(PH_3)_2$, these HOMO and LUMO interact with antibonding and bonding combinations of H 1s orbitals, respectively. Consequently a decrease in electron density in the d_{yz} orbital and an increase in the Pt s–p-hybridized orbital take place, as is seen in the gross population in Table I. In contrast to the trans compound, the switching between an occupied and a vacant orbital does not take place in the cis compound.

In transition-metal chemistry the electron count on the hydride is usually presumed to be 2 and molecular structures and reactions are interpreted on the basis of this presumption. However, the gross population asserts almost neutral H ligands in both Pt-$(H)_2(PH_3)_2$ and $Pt(H)(CH_3)(PH_3)_2$ complexes; the net charge on H in Table I is between +0.05 and −0.03, to be compared with Noell and Hay's +0.02.[24a] The net charge on Pt from the Mulliken population analysis is −0.23 to −0.67 in Table I and −0.45 in Noell and Hay's. These negative charges are in conflict with an intuition for an oxidized Pt compound. This is a defect of the population analysis. In fact Noell and Hay found a positive charge of +1.22 in a modified analysis.

The bonding schemes in *cis*-$Pt(H)(CH_3)(PH_3)_2$ and *trans*-$Pt(H)(CH_3)(PH_3)_2$ are essentially the same as in *cis*-$Pt(H)_2(PH_3)_2$ and *trans*-$Pt(H)(CH_3)(PH_3)_2$, respectively, although the molecular symmetry is lower here. Mulliken populations for the hydride methyl compounds are given in the Table I. One notes that the

(37) Pearson, R. G. *Acc. Chem. Res.* **1971**, *4*, 152.

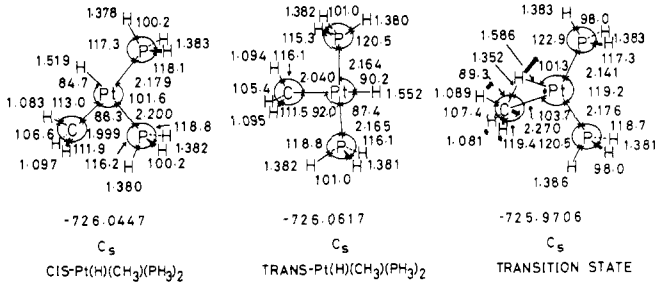

Figure 3. Fully optimized geometries (in Å and deg) of *cis*-$Pt(H)(CH_3)(PH_3)_2$, *trans*-$Pt(H)(CH_3)(PH_3)_2$, and the transition state with their total energies in the smaller basis set. Arrows in the transition state show the reaction coordinate vectors.

Table II. Calculated and Observed PtP Bond Distances (Å)

	basis	
	smaller	larger[a]
Calculated		
$Pt(PH_3)_2$	2.154	2.175
cis-$Pt(H)_2(PH_3)_2$	2.194	2.242
trans-$Pt(H)_2(PH_3)_2$	2.166	2.182
cis-$Pt(H)(CH_3)(PH_3)_2$	2.179	
trans-$Pt(H)(CH_3)(PH_3)_2$	2.164	
	2.165	
Observed		
$Pt[PPh(t\text{-}Bu)_2]_2$[b]	2.252	
$[Pt(t\text{-}Bu)_2P(CH_2)_3P(t\text{-}Bu)_2]_2$[c]	2.270	
$PtCl_2[(t\text{-}Bu)_2P(CH_2)_3P(t\text{-}Bu)_2]$[c]	2.281	
$PtO_2[PPh(t\text{-}Bu)_2]_2$[d]	2.290	
cis-$PtCl_2[P(CH_3)_3]_2$[e]	2.239	
trans-$PtCl_2[P(C_2H_5)_3]_2$[f]	2.300	
trans-$Pt(H)(Cl)[PPh_2(C_2H_5)]_2$[g]	2.268	

[a] Reference 26. [b] Reference 3. [c] Reference 5. [d] Reference 17. [e] Reference 39. [f] Reference 40. [g] Reference 41.

Pt–C overlap population is smaller than the corresponding Pt–H population.

(B) Equilibrium Geometries. The calculated equilibrium geometries are given in Figures 2a and 3. We did not assume any symmetry of the complexes except C_s, which was necessary for stopping a rather free internal rotation of PH_3 groups. The geometry optimization resulted in D_{2d}, C_{2v}, and C_{2h} symmetries for $Pt(PH_3)_2$, *cis*-$Pt(H)_2(PH_3)_2$, and *trans*-$Pt(H)_2(PH_3)_2$, respectively. All the vibrational frequencies except for the near-zero PH_3 rotational frequencies are found to be real, confirming that these are in fact equilibrium geometries. The linear structure of $Pt(PH_3)_2$ is expected from a Walsh diagram for ML_2 transition-metal complexes with a d^{10} electron configuration.[38] The X-ray structural analysis has actually revealed the PPtP bond angle of 177° in $Pt[PPh(t\text{-}Bu)_2]_2$.[3] The square-planar structures of *cis*- and *trans*-$Pt(H)_2(PH_3)_2$ are reasonable, since four-coordinate platinum(II) complexes have been well-known to take a square-planar structure.[6]

The calculated HPt bond lengths range from 1.519 to 1.563 Å (Figures 2a and 3), with which there is no experimental structural data to compare. The relativistic ECP calculation on the PtH diatomic molecule gives the bond length of 1.462 Å,[24a] whereas it is experimentally known as 1.528 Å.[29] This suggests that our calculations also underestimate the bond length by about 0.07 Å.

The calculated PtP bond distances are compared in Table II with known experimental values. The calculated values of

(38) Pearson, R. G. *J. Am. Chem. Soc.* **1969**, *91*, 4947.
(39) Messmer, G. G.; Amma, E. L.; Ibers, J. A. *Inorg. Chem.* **1967**, *6*, 725.
(40) Messmer, G. G.; Amma, E. L. *Inorg. Chem.* **1966**, *5*, 1775.
(41) Eisenberg, R.; Ibers, J. A. *Inorg. Chem.* **1965**, *4*, 773.
(42) Shimanouchi, T. "Tables of Molecular Vibrational Frequencies"; National Bureau of Standards: Washington, DC, 1972; Vol. I, NSRDS-NBS 39, p 16.

Table III. Vibrational Frequencies of H_2, PH_3, $Pt(PH_3)_2$, *cis*- and *trans*-$Pt(H)_2(PH_3)_2$, and the Transition State[a]

H_2[b] + PH_3	$Pt(PH_3)_2$	transitn state[c]	$Pt(H)_2(PH_3)_2$[d] cis	trans	sym and assignt for *cis*-$Pt(H)_2(PH_3)_2$[e]
	160	150 (140)	150	190	A_1 PPtP b (in-plane)
	410	400 (400)	380	410	A_1 PtP s (sym)
	390	440 (410)	390	400	B_1 PtP s (anti)
	180	170 (170)	470	210	A_2 PPtP b (out-of-plane)
	560	600 (580)	610	630	A_2 PtPH b (anti out-of-plane)
	560	640 (630)	640	670	B_1 PtPH b (anti in-plane)
	630	710 (700)	730	730	A_1 PtPH b (sym in-plane)
	630	610 (600)	760	680	B_2 PtPH b (sym out-of-plane)
		530 (380)	920	880	B_2 HPtH b (out-of-plane)
			920	920	B_1 HPtP b
		330 (250)	1160	1090	A_1 HPtH b (in-plane)
1430 [992]	1240	1280 (1280)	1270	1260	B_1 HPH b (a_1)
	1260	1310 (1310)	1300	1260	A_1 HPH b (a_1)
1540 [1118]	1400	1420 (1420)	1420	1390	B_1 HPH b (e)
	1400	1430 (1430)	1420	1390	A_2 HPH b (e)
1540 [1118]	1410	1440 (1440)	1420	1400	A_1 HPH b (e)
	1410	1440 (1440)	1420	1400	B_2 HPH b (e)
			2140	1810	B_1 PtH s (anti)
		360i (270i)	2210	2150	A_1 PtH s (sym)
3100 [2323]	3050	3050 (3050)	3060	3070	A_1 PH s (a_1)
	3050	3060 (3060)	3060	3070	B_1 PH s (a_1)
3150 [2328]	3080	3080 (3080)	3090	3100	A_2 PH s (e)
	3080	3080 (3080)	3090	3100	B_2 PH s (e)
3150 [2328]	3090	3100 (3100)	3120	3110	A_1 PH s (e)
	3100	3100 (3100)	3120	3120	B_1 PH s (e)
4660 (3300)		4150 (2940)			A_1 HH s

[a] The force constant matrix is obtained at the smaller basis RHF level. Vibrational modes corresponding to internal rotation of PH_3 are excluded. [b] Values in square brackets are experimental fundamental frequencies for gaseous PH_3.[42] A values in parentheses is a calculated frequency of D_2. [c] Vibrational frequencies of $Pt(D)_2(PH_3)_2$ are given in parentheses. Three near-zero frequencies are not given. Two of these correspond to PH_3 rotation, and the third corresponds to H_2 out-of-plane translational mode. [d] Two near-zero frequencies corresponding to PH_3 rotations are not given. [e] The b and s means bending and stretching, respectively. For modes within PH_3 ligands irreducible representation in C_{3v} symmetry is given in parentheses.

2.15–2.20 Å, regardless whether we use a smaller (STO-2G) or a larger (LP-31G) basis set for P, are about 0.1 Å shorter than 2.2–2.3 Å, the observed values for many Pt phosphine compounds.[6] This is probably due to the inadequancy of the Pt ECP parameters adopted in the calculation. The poor basis set used for P and the lack of correlation effect may also be responsible for this error.

Noell and Hay reported optimized HPt distance and HPtH and PPtP bond angles of *cis*- and *trans*-$Pt(H)_2(PH_3)_2$ by the energy-only method with a fixed PtP bond distance of 2.268 Å.[24b] Their HPt bond distances of 1.55 and 1.61 Å in the cis and trans compounds, respectively, are about 0.04 Å longer than those of the present work. Concerned with this difference, we have carried out a full geometry optimization for *cis*-$Pt(H)_2(PH_3)_2$ by using the ECP parameters and the basis set used by them.[24b] The result, shown in the second column of Figure 2b, gives the HPt distance of 1.51 Å, in agreement with the present work, and the PPt distance of 2.51 Å, much longer than the present results and those observed in experiments.

The HPt bond length becomes shorter as the trans-positioned ligand is switched from CH_3 to H and from H to PH_3. The same trend is found for the PPt and the CPt bond lengths. From this fact, one can deduce the trans influence order $H^- > CH_3^- > PH_3$. The trans influence order will also be discussed in section E.

Table IV. Vibrational Frequencies of CH_4, *cis*-$Pt(H)(CH_3)(PH_3)_2$, *trans*-$Pt(H)(CH_3)(PH_3)_2$, and the Transition State[a]

CH_4[b]	$Pt(H)(CH_3)(PH_3)_2$ cis[c]	trans	transitn state[c]	symm and assignt for *cis*-$Pt(H)(CH_3)(PH_3)_2$[d]
	160 (160)	120	120 (120)	A″ PPtC b (out-of-plane)
	170 (170)	160	100 (100)	A′ PPtP b (in-plane)
	250 (250)	230	150 (150)	A′ PPtC b (in-plane)
	370 (370)	400	370 (370)	A′ PtP s (sym)
	400 (400)	400	400 (400)	A′ PtP s (anti)
	490 (410)	600	430 (350)	A″ PPtH b (out-of-plane)
	560 (560)	520	520 (520)	A′ PtC s
	640 (640)	630	580 (570)	A″ PtPH b (anti out-of-plane)
	680 (670)	690	640 (640)	A′ PtPH b (anti in-plane)
	720 (720)	740	720 (720)	A′ PtPH b (sym in-plane)
	780 (680)	690	620 (610)	A″ PtPH b (sym out-of-plane)
	870 (870)	900	1080 (970)	A″ PtCH b (out-of-plane)
	940 (940)	880	1090 (980)	A′ PtCH b (in-plane)
	1150 (840)	1070	1030i (810i)	A′ HPtC b (in-plane)
	1260 (1260)	1240	1290 (1290)	A′ HPH b (a_1)
	1290 (1290)	1260	1320 (1320)	A′ HPH b (a_1)
	1410 (1410)	1390	1420 (1420)	A″ HPH b (e)
	1410 (1410)	1390	1430 (1430)	A′ HPH b (e)
	1410 (1410)	1400	1430 (1430)	A′ HPH b (e)
	1410 (1410)	1400	1440 (1440)	A″ HPH b (e)
1520 (1150) T_2	1440 (1440)	1450	1450 (1450)	A′ HCH b (a_1)
1740 (1230) E	1660 (1660)	1670	1630 (1530)	A′ HCH b (e)
	1690 (1690)	1680	1680 (1680)	A″ HCH b (e)
	2160 (1530)	2030	2170 (1710)	A′ PtH s
	3040 (3040)	3060	3120 (3120)	A′ PH s (a_1)
	3060 (3060)	3060	3030 (3030)	A′ PH s (a_1)
3190 (2250) A_1	3070 (3070)	3080	3060 (3060)	A′ CH s (a_1)
	3070 (3070)	3090	3060 (3060)	A″ PH s (e)
	3090 (3090)	3090	3070 (3070)	A″ PH s (e)
3280 (2430) T_2	3090 (3090)	3100	3090 (3090)	A″ CH s (e)
	3100 (3100)	3100	3160 (3160)	A′ PH s (e)
	3110 (3110)	3110	3240 (3240)	A′ PH s (e)
	3240 (3240)	3120	3290 (3290)	A′ CH s (e)

[a] Based on the force constants obtained at the smaller basis RHF level. Three near-zero frequencies corresponding to internal rotations of PH_3 and CH_3 are excluded. [b] Values in parentheses are calculated CD_4 frequencies. The irreducible representations are those in T_d symmetry. [c] Vibrational frequencies of $Pt(D)(CH_3)(PH_3)_2$ are given in parentheses. [d] The b and s means bending and stretching, respectively. For modes within PH_3 and CH_3 ligands irreducible representation in C_{3v} is given in parentheses.

The HPtH bond angle in the cis dihydride complex is calculated to be 81.8°, smaller than 90°, while the PPtP angle is 104.4°, larger than 90°. This is in agreement with the Hückel calculations for the R_2ML_2 transition-metal complexes.[19] The ligand–ligand steric repulsion is expected to be the smallest in case of PH_3 among substituted bulky phosphines. Therefore, the calculated bond angle is considered to be electronically optimum for phosphines that have the same basicity as PH_3.

(C) Vibrational Frequencies. All the vibrational modes of $Pt(PH_3)_2$, *cis*-$Pt(H)_2(PH_3)_2$, *trans*-$Pt(H)_2(PH_3)_2$, *cis*-$Pt(H)(CH_3)(PH_3)_2$, and *trans*-$Pt(H)(CH_3)(PH_3)_2$ are obtained from force constant matrices calculated by a numerical differentiation

Table V. Calculated and Observed PtH Stretching Frequencies (cm^{-1})[a]

	anti sym	sym
Calculated		
trans-$Pt(H)_2(PH_3)_2$	1810 (1290[d])	2150 (1520[d])
cis-$Pt(H)_2(PH_3)_2$	2140 (1520[d])	2210 (1570[d])
trans-$Pt(H)(CH_3)(PH_3)_2$	2030	
cis-$Pt(H)(CH_3)(PH_3)_2$	2160	
Observed		
trans-$Pt(H)_2[P(i\text{-}Pr)_3]_2$[b]	1735	
trans-$Pt(H)_2[P(c\text{-}C_6H_{11})_3]_2$[b]	1710 (1230[d])	
trans-$Pt(H)_2[PPh(t\text{-}Bu)_2]_2$[b]	1780	
trans-$Pt(H)_2[P(C_2H_5)_3]_2$[b]	1725	
cis-$Pt(H)_2[(t\text{-}Bu)_2P(CH_2)_3P(t\text{-}Bu)_2]$[c]	1995 (1430[d])	
cis-$Pt(H)_2[(t\text{-}Bu)_2P(CH_2)_2P(t\text{-}Bu)_2]$[c]	1980, 2008	
cis-$Pt(H)_2[Men_2P(CH_2)_2PMen_2]$[c]	1989	
cis-$Pt(H)_2$[Men(Ph)$P(CH_2)_2P$(Ph)-Men][c]	1977, 2004	
cis-$Pt(H)_2[t\text{-}Bu(Ph)P(CH_2)_2P(Ph)t\text{-}Bu]$[c]	1985	
cis-$Pt(H)_2[Ph_2P(CH_2)_2PPh_2]$[c]	1930	

[a] At RHF level with the smaller basis set. [b] Reference 4. [c] Reference 5. [d] In a deuterated compound $Pt(D)_2L_2$.

Table VI. Calculated and Observed PtC Stretching Frequencies (cm^{-1})[a]

Calculated	
trans-$Pt(H)(CH_3)(PH_3)_2$	520
cis-$Pt(H)(CH_3)(PH_3)_2$	560
Observed	
trans-$Pt(X)(CH_3)(PH_3)_2$[b]	
X = NO_3	566
X = NC	556
X = Cl	551
X = Br	548
X = NO_2	544
X = I	540
X = CN	516
cis-$Pt(Cl)(CH_3)(PH_3)_2$[b]	516

[a] See the footnote *a* of Table V. [b] Reference 43.

of the analytical energy gradients. Calculated normal vibrational frequencies and their assignments, excluding near-zero frequencies of CH_3 and PH_3 rotations, are shown in Tables III and IV. Experimentally observed PtH and PtC stretching fundamental frequencies are compared in Tables V and VI, respectively, with the calculated normal-mode frequencies.

The agreement is generally very good for both PtH and PtC stretchings with the calculated values overestimating the observed values by 4–8%. Both experimentally and theoretically, the antisymmetric PtH stretching for the cis dihydride compound is found to have a higher frequency than the trans compound by over 200 cm^{-1}. For the hydride methyl compound the calculation similarly predicts a higher PtC stretching frequency for cis than for trans. These results can be interpreted as an indication that the hydride shows a stronger trans influence than PH_3. In the experiment for $Pt(CH_3)Cl(PEt_3)_2$, trans has a higher PtC frequency than cis, reflecting a weaker trans influence of Cl.

Vibrational modes originating from PH_3 ligands, namely, HPH bending (calculated 1240–1540 cm^{-1}) and PH stretching (calculated 3050–3150 cm^{-1}) are up to 40% too large, as expected from this small STO-2G basis set for P. However, one can clearly recognize a decrease of these frequencies upon coordination to the Pt atom and a subsequent slight reversal upon oxidative addition.

There are many vibrational modes whose frequencies are about 1000 cm^{-1} or less. These frequencies have not yet been identified experimentally. The present calculation predicts about 900 and 1000–1200 cm^{-1} for the HPtH out-of-plane and in-plane motions, respectively. However, it should be remembered that the present level of calculations is expected to overestimate experimental frequencies by 5–15%.[44] Both of these frequencies in *cis*-$Pt(H)_2(PH_3)_2$ are larger than those in *trans*-$Pt(H)_2(PH_3)_2$. Bending and stretching modes involving a PtP bond occur at 700 cm^{-1} or less. These frequencies are less accurate than those involving a PtH bond, because of the minimal (STO-2G) PH_3 basis set.

Table VII. Calculated Relative Energy for $Pt(PH_3)_2 + H_2 \rightarrow Pt(H)_2(PH_3)_2$ (in kcal/mol)[a]

method	$Pt(PH_3)_2 + H_2$[b]	transition state	$Pt(H)_2(PH_3)_2$ cis	$Pt(H)_2(PH_3)_2$ trans
RHF	0	+5.2	−36.9	−38.0
SD–CI	0	+8.7	−27.0	−25.1
SD–CI + QC	0	+7.3	−26.8	−24.0
SD–CI + QC + ZPC	0	+8.2	−21.5	−20.3

[a] The larger basis set. [b] RHF energy for $Pt(PH_3)_2$ = −43.615 21 hartree and for H_2 = −1.122 95 hartree. SD–CI correlation energy = −0.298 19 and −0.024 76 hartree. QC = −0.041 93 and −0.000 34 hartree. ZPC = 43.2 and 6.7 kcal/mol.

Table VIII. Calculated Relative Energy for $Pt(PH_3)_2 + CH_4 \rightarrow Pt(H)(CH_3)(PH_3)_2$ (in kcal/mol)[a]

method	$Pt(PH_3)_2 + CH_4$[b]	transitn state	$Pt(H)(CH_3)(PH_3)_2$ cis	$Pt(H)(CH_3)(PH_3)_2$ trans
RHF	0	22.6	−15.0	−17.5
SD–CI	0	35.3	1.2	1.2
SD–CI + QC	0	29.6	−4.7	−3.9
SD–CI + QC + ZPC	0	28.2	−4.5	−3.5

[a] The larger basis set. [b] RHF energy for CH_4 = −39.976 88 hartree. SD–CI correlation energy = −0.112 68 hartree. QC = −0.005 24 hartree. ZPC = 30.1 kcal/mol.

(D) Relative Stability of Four-Coordinate Cis and Trans Platinum(II) Compounds. In the oxidative addition reaction of H_2 to platinum(0) diphosphine only the trans isomer has been found as a product. The relative stability of cis and trans isomers could be a determining factor for this selectivity.[45] We have calculated the energy of the two structures relative to the reactant by the RHF and the SD – CI + QC method with a larger basis set for the RHF-optimized geometries. CI calculations give the coefficient of the RHF configuration of about 0.924–0.930 for all the Pt complexes studied, supporting qualitative discussions on electronic structures based on an RHF wave function. The zero-point energy correction (ZPC) has been calculated with the vibrational frequencies in Tables III and IV and therefore is probably overestimated. The results with ZPC are shown in the last two columns of Tables VII and VIII for $Pt(H)_2(PH_3)_2$ and $Pt(H)(CH_3)(PH_3)_2$, respectively.

In our best calculation (SD – CI + QC + ZPC) the energy differences between cis and trans compounds both in Tables VII and VIII are less than a few kilocalories per mole, which is within the error limit of the present level of calculation. This means that no obvious thermodynamical preference of the trans compound has been found in our model compound $Pt(H)_2(PH_3)_2$. The trans selectivity found experimentally will be explained later in terms of a steric repulsion between bulky phosphines.

The difference in the principal mode of reaction, i.e., the oxidative-addition reaction for H_2 vs. the reductive-elimination reaction for CH_4, can be understood easily in terms of the difference in exothermicity, calculated in Tables VII and VIII. For H_2, the addition product is more stable than the two-coordinate reactant by about 20 kcal/mol, making the addition reaction more favorable. For CH_4, the reaction is found to be essentially thermoneutral, and the entropy factor should favor the elimination product. As discussed in the following, the exact exothermicity is hard to evaluate. However, the qualitative difference in behavior between H_2 and CH_4 should be meaningful.

(43) Adams, D. M.; Chatt, J.; Shaw, B. L. *J. Chem. Soc.* **1960**, 2047.

(44) Hamada, Y.; Tanaka, N.; Sugawara, Y.; Hirakawa, A. Y.; Tsuboi, M.; Kato, S.; Morokuma, K. *J. Mol. Spectrosc.* **1982**, *96*, 313.

(45) Glasstone, S.; Laider, K. J.; Eyring, H. "The Theory of Rate Processes"; McGraw-Hill: New York, 1941.

Table IX. Bond Strength, Bond Distance, Stretching Frequency, and Overlap Population of PtH, PtC, and PtP

	$Pt(PH_3)_2$	$Pt(H)_2(PH_3)_2$		$Pt(H)(CH_3(PH_3)_2$	
		cis	trans	cis	trans
		Bond Strength (kcal/mol)			
PtH		70[a]	61[a]	(70)[d]	(65)[d]
PtC				(34)[e]	(41)[e]
PtP	40[b]	38[c]	45[c]		
		Bond Distance (Å)			
PtH		1.522	1.563	1.519	1.552
PtC					
PtP	2.154	2.194	2.166	2.179, 2.200	2.164, 2.165
		Stretching (cm^{-1})			
PtH		2140, 2210	1810, 2150	2160	2030
PtC				560	520
PtP	390, 400	380, 390	400, 410	370, 400	400
		Bond Population			
PtH		0.39	0.38	0.39	0.38
PtC				0.32	0.29
PtP	0.35	0.26	0.33	0.25	0.33

[a] $[E(Pt(PH_3)_2) + 2E(H) - E(Pt(H)_2(PH_3)_2)]/2$. [b] $E(PtPH_3) + E(PH_3) - E(Pt(PH_3)_2)$. [c] $E(Pt(H)_2PH_3) + E(PH_3) - E(Pt(H)_2(PH_3)_2)$. [d] Assumed value. See Text. [e] $E(Pt(PH_3)_2) + E(H) + E(CH_3) - E(Pt(H)(CH_3)(PH_3)_2) - E_A(PtH)$, where $E_A(PtH)$ is the assumed value of PtH bond strength.

Noell and Hay calculated the stabilization energies[24a] of *cis*-$Pt(H)_2(PH_3)_2$ and *trans*-$Pt(H)_2(PH_3)_2$ relative to the $Pt(PH_3)_2 + H_2$ system and obtained from the RHF calculation the energies of 6.7 and 10.6 kcal/mol, respectively, which are about 30 kcal/mol less than those of 36.9 and 38.0 kcal/mol at the RHF level of calculation in the present work. The dissociation energy, D_e, of the ground state of the PtH molecule is to be 53.4 kcal/mol in their basis set and ECP[24a] while to be 65.0 kcal/mol in the present set and ECP. The difference of 12 kcal/mol per each PtH bond will explain a main part of the stabilization energy difference. Because the dissociation energy of the PtH molecule has not been known experimentally, we cannot determine which result is more reasonable. It is noted, however, that the calculated vibrational frequency of PtH molecule is 2260 cm^{-1} in the present calculation and is in better agreement with the observed value of 2377 cm^{-1} than that of 2009 cm^{-1} by Noell and Hay.[24a]

(E) Nature of PtH, PtC, and PtP Bonds. A comparison between cis and trans conformers of $Pt(H)_2(PH_3)_2$ and $Pt(H)(CH_3)(PH_3)_2$ gives interesting features of PtH, PtC, and PtP bonds. In Table IX, we have compared the bonding characteristics such as estimated bond strength, bond distance, stretching frequency, and bond population among the compounds we studied. The PtH bond strength is calculated to be half the energy difference between $Pt(PH_3)_2 + H + H$ and $Pt(H)_2(PH_3)_2$ and the PtP bond strength to be an energy difference between $Pt(H)_2(PH_3) + PH_3$ and $Pt(H)_2(PH_3)_2$. The calculated PtH bond strength is 70 and 61 kcal/mol for *cis*- and *trans*-$Pt(H)_2(PH_3)_2$, respectively. Even though a direct comparison with experiments cannot be made, it is interesting to note that Beauchamp et al. and Ridge et al. estimated the metal cation–hydride bond energy to be in the range of 50–80 kcal/mol for Cr, Mn, Fe, Co, Ru, and Rh complexes.[46,47] Halpern also estimated a bond dissociation energy of MH as ~60 kcal/mol[48] and that of MC as 20–30 kcal/mol.[49] We find that the PtH bond in the cis compound has a larger bond strength, a shorter distance, a larger vibrational frequency, and a larger bond population than those in the trans compound. To the contrary, the PtP bond in the cis product has a smaller bond strength, a longer distance, lower vibrational frequencies, and a smaller bond population. The PtH bond in cis appears to be stronger than in trans, whereas the PtP bond in cis is weaker. These results can be explained by a difference in the so-called trans influence; the trans influence of H is stronger than that of PH_3. This is also consistent with a longer PtCl bond distance of 2.42 Å in *trans*-$Pt(H)(Cl)[PPh_2(C_2H_5)]_2$,[39] where H is in the trans position to Cl, than that of 2.37 Å in *cis*-$PtCl_2[P(CH_3)_2]_2$,[41] where phosphine is in the trans position to Cl.

In *cis*-$Pt(H)(CH_3)(PH_3)_2$, both of PtH and PtC bonds have smaller bond distances, larger stretching frequencies, and larger bond populations than those in the corresponding trans compound. These results suggest that the trans influence of a CH_3 ligand is larger than that of PH_3 ligand. In the trans dihydride the PtH bond distance is larger than that in trans hydride methyl compound, indicating a smaller trans influence of CH_3 than H.

In order to estimate the PtC bond strength, we first calculated the stabilization energy of *cis*- and *trans*-$Pt(H)(CH_3)(PH_3)_2$ relative to $Pt(PH_3)_2 + H + CH_3$ to be 104 and 106 kcal/mol, respectively. If we assume and subtract the PtH bond strength of 70 and 65 kcal/mol, respectively, we obtain an estimate of the PtC bond strength to be 34 and 41 kcal/mol for *cis*- and *trans*-$Pt(H)(CH_3)(PH_3)_2$, respectively. The assumed PtH bond length of the cis compound is that of *cis*-$Pt(H)_2(PH_3)_2$ and is probably reasonable because in both of them the ligand trans to hydride is a phosphine. The assumed PtH bond strength of 65 kcal/mol for *trans*-$Pt(H)(CH_3)(PH_3)_2$ is an average of the PtH bond strengths in *cis*- and *trans*-$Pt(H)_2(PH_3)_2$ and is deduced from the fact that a ligand trans to hydride is CH_3 in *trans*-$Pt(H)(CH_3)(PH_3)_2$ and that a trans influence of CH_3 group is weaker than hydride and stronger than phosphine. The estimated PtC bond strengths of 34 and 41 kcal/mol are in good agreement with a range of values of 20–30 kcal/mol[49] for metal–alkyl bond dissociation energies of coordinately saturated cobalt compounds and a value of 41 kcal/mol[46] for the Co–CH_3 bond obtained from ion-beam studies.

Transition States for Oxidative Addition of H_2 to $Pt(PH_3)_2$ and Reductive Elimination of CH_4 from $Pt(H)(CH_3)(PH_3)_2$. (A) Transition State for $H_2 + Pt(PH_3)_2 \rightarrow Pt(H)_2(PH_3)_2$. We have found a transition state for the reaction $H_2 + Pt(PH_3)_2 \rightarrow Pt(H)_2(PH_3)_2$ and shown its geometry in the last column in Figure 2a. In the search of the transition state C_s symmetry is assumed to restrict rather free rotations of PH_3 around metal–phosphorus bonds. The resultant transition state has C_{2v} symmetry. Normal-mode frequencies of the transition state are given in Table III where near-zero vibrational frequencies are not included.

Relative energies of the transition state in various approximations are given in Table VII. Our best calculation (CI + QC) gives a classical barrier height of 7 kcal/mol. The zero-point energy correction (ZPC) changes the effective barrier to 8 kcal/mol. Though these values should be taken to be only semiquantitative, it is safe to say that the barrier for this model reaction is low, consistent with the experimental fact[4,5] that the oxidative addition of H_2 takes place easily.

The geometry of the transition state resembles that of the reactants; the HH bond length of 0.77 Å is only 4% longer than 0.73 Å in the H_2 molecule, the PPtP angle of 148° is not far from 180° of the reactant $Pt(PH_3)_2$. On the other hand, the newly formed PtH distance is still substantially longer than that in the product. The transition state for the oxidative addition is, therefore, characterized as "an early transition state".

In a kinetic study of hydrogen and deuterium addition reaction of $IrCl(CO)(PPh_3)_2$, it has been suggested[50] on the basis of a small kinetic isotope effect[9] that the HH bond stretch is small at the transition state. The present result is consistent with this suggestion. Dedieu and Strich also suggested small HH stretching in the transition state based on their extended Hückel study of

(46) Armentrout, P. B.; Beauchamp, J. L. *J. Am. Chem. Soc.* **1981**, *103*, 784.

(47) (a) Foster, M. S.; Beauchamp, J. L. *J. Am. Chem. Soc.* **1975**, *97*, 4808. (b) Stevens, A. E.; Beauchamp, J. L. *J. Am. Chem. Soc.* **1981**, *103*, 190. (c) Armentrout, P. B.; Beauchamp, J. L. *J. Chem. Phys.* **1981**, *74*, 2819; *J. Am. Chem. Soc.* **1980**, *102*, 1736. (d) Allison, J.; Freas, R. B.; Ridge, D. P. *J. Am. Chem. Soc.* **1979**, *101*, 1332. (e) Allison, J.; Ridge, D. P. *J. Am. Chem. Soc.* **1979**, *101*, 4998. (f) Dietz, T. G.; Chatellier, D. S.; Ridge, D. P. *J. Am. Chem. Soc.* **1978**, *100*, 4905.

(48) Halpern, J. *Pure Appl. Chem.* **1979**, *51*, 2171.

(49) Halpern, J. *Acc. Chem. Res.* **1982**, *15*, 238.

(50) Collman, J. P.; Roper, W. R. *Adv. Organomet. Chem.* **1968**, *7*, 53.

Table X. Analysis of Kinetic Deuterium Isotope Effect at 300 K for the Oxidative-Addition Reaction $(X)_2 + Pt(PH_3)_2 \rightarrow Pt(X)_2(PH_3)_2$ (X = H and D)[a]

	reactant		transitn state		
sym	assignt[b] or ν, cm^{-1}	R_i	ν,[b] cm^{-1}	R_i^*	$R_i^* R_i^{-1}$
A_1	$t(x)$	1.0	360i	1.31	1.31
	610	1.0	710	0.99	0.99
	4660	0.054	4160	0.077	1.43
A_2	$r(x)$	1.0	530	0.89	0.89
	580	1.0	600	0.98	0.98
B_1	$t(z)$	1.0	330	0.96	0.96
	$r(y)$	1.0	440	0.98	0.98
B_2	$t(y)$	1.0		(1.0)[c]	(1.0)[c]
total[d]		0.054		0.061	1.48

[a] Only factors contributing significantly to the isotope effect are listed. [b] The $t(i)$ is a translation of X_2 to the i direction, and the $r(i)$ is the rotation of X_2 around i axis based on the coordinate system in Scheme I. Frequencies are those in dihydride compound $Pt(H)_2(PH_3)_2$. [c] Assumed value. See text. [d] Total product of contributions of all the modes where R_i and R_i^* for PH_3 rotations having near-zero frequencies are assumed to be 1.

$RhCl(PH_3)_3 + H_2$.[20] Noell and Hay,[24a] however, reported a large HH stretch in their ab initio calculation, which suggests a large isotope effect. We have calculated the kinetic deuterium isotope effect r at 300 K using the Bigeleisen equation[51]

$$r = \frac{k_1}{k_2}\frac{s_2 s_1^*}{s_1 s_2^*}\frac{\kappa_2}{\kappa_1} = R_L^*\left(\prod_i^{3N-7} R_i^*\right)\left(\prod_i^{3N-6} R_i\right)^{-1} \quad (1)$$

$$R_L^* \equiv \frac{\nu_{1L}^*}{\nu_{2L}^*} \quad (2)$$

$$R_i^a \equiv \frac{u_{1i}^a}{u_{2i}^a}\frac{\exp(-u_{1i}^a/2)\{1-\exp(-u_{1i}^a)\}^{-1}}{\exp(-u_{2i}^a/2)\{1-\exp(-u_{2i}^a)\}^{-1}} \quad (3)$$

$$a = \text{none or } *$$

$$u_i \equiv h\nu_i/kT$$

where s is the symmetry number, κ is the transmission coefficient, ν_i is the ith vibrational frequency of the reactants, ν_i^* is that of the transition state, ν_L^* is the reaction-coordinate frequency, and subscripts 1 and 2 refer to the hydride and its deuterated systems, respectively.

The calculated isotope ratio r is 1.48, consistent with the experimental values of 1.2–1.3.[9] Analysis of the isotope ratio is given in Table X where only factors giving R values substantially different from unity are shown. The largest contributions to the isotope ratio r are 1.43 from the weakening of the XX bond (X = H and D) at the transition state and 1.31 from the reaction coordinate, i.e., the translational displacement of X_2 approaching Pt. Other modes contribute to moderate the effect of these two factors. In our calculation the contribution of the out-of-plane B_2 bending has been assumed to be unity because of numerical errors introduced in calculating this small vibrational frequency. However, its real effect is expected to reduce the isotope ratio, making the calculated value even closer to the experimental value.

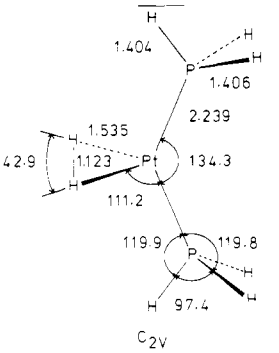

Figure 4. Fully optimized geometry (in Å and deg) of the "transition state" leading directly to a trans compound found by forcing the H_2 bond axis perpendicular to the PPtP plane with an overall C_{2v} symmetry. The state is unstable to the H_2 rotation around the C_{2v} symmetry axis and therefore is not a true transition state. The smaller basis set.

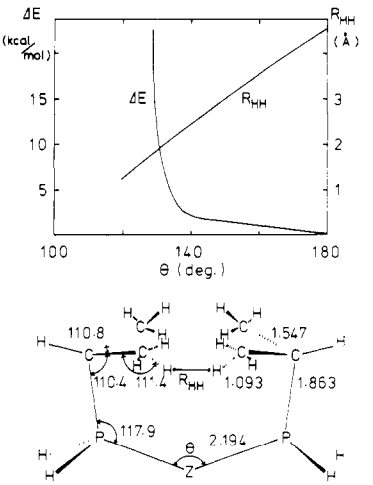

Figure 5. Steric repulsion energy (ΔE in kcal/mol) between two PH_2-(*i*-Pr) molecules and the nearest HH distance (R_{HH} in Å) between two isopropyl groups. The smaller basis set.

The transition-state geometry seems reasonable judged from the calculated low activation energy and small deuterium kinetic isotope effect. However, it may be suspected that Pt ECP parameters[29] used in the present work may suffer a same defect as a similar ECP showed in an unrealistic attractive potential curve for the dichlorine molecule.[59] In order to test ECP and basis set dependency, we fully optimized the geometry of the transition state using more reliable Pt ECP parameters and the basis set of Noell and Hay[24b] and have shown the result in the last column of Figure 2b. The transition state is apparently "an early one"; namely, the HH distance of 0.77 Å is only a 5% increase from that of 0.731 Å in a free H_2 molecule, and the HPt distance of 2.01 Å is much longer than that of 1.51 Å in the product *cis*-$Pt(H)_2(PH_3)_2$. The calculated activation energy is small, 10.0 kcal/mol at the RHF level, and is comparable with the present value of 5.2 kcal/mol. From these results it can be concluded that the earliness and the low activation energy is not likely to be an artifact of the ECP parameters and basis functions. The rather "late" transition state obtained in a GVB calculation by Noell and Hay[24a] may be due to incomplete optimization of the geometry.

The transition state found at present work is apparently on the way to the cis product. We also searched a transition state leading directly to a trans product. In this search the C_{2v} symmetry is enforced by keeping the HH bond axis perpendicular to the PPtP plane. The "transition state" thus found, shown in Figure 4, has an activation energy of about 50 kcal/mol at the RHF level, much higher than the activation energy of several kilocalories per mole

(51) Bigeleisen, J.; Mayer, M. G. *J. Chem. Phys.* **1947**, *15*, 261.
(52) (a) Parshall, G. W. *Acc. Chem. Res.* **1970**, *3*, 139. (b) Bruce, M. I. *Angew. Chem., Int. Ed. Engl.* **1977**, *16*, 73. (c) Omae, I. *Coord. Chem. Rev.* **1980**, *32*, 235.
(53) Halpern, J. *Adv. Catal.* **1959**, *11*, 301.
(54) Osborn, J. A.; Jardine, F. H.; Wilkinson, G. *J. Chem. Soc. A* **1966**, A1711.
(55) Nyholm, R. S. *Proc. Int. Congr. Catal. 3rd, 1964 (1965)* 25.
(56) Kitaura, K.; Morokuma, K. *Int. J. Quantum Chem.* **1976**, *10*, 325.
(57) Hoyano, J. K.; McMaster, A. D.; Graham, W. A. G. *J. Am. Chem. Soc.* **1983**, *105*, 7190.
(58) Wax, M. J.; Stryker, J. M.; Buchanan, J. M.; Kovac, C. A.; Bergman, R. G. *J. Am. Chem. Soc.* **1984**, *106*, 1121.
(59) Hay, P. J.; Wadt, W. R.; Kahn, L. R. *J. Chem. Phys.* **1978**, *68*, 3059.

Scheme II

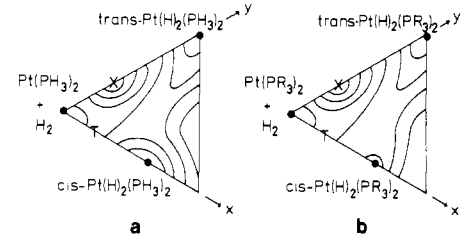

of the path leading to a cis product. This "transition state", however, is found to have two negative force constants, one for the reaction and another for the HH rotation around the C_{2v} axis, and, therefore, is not a true transition state. The reactants trying to follow this path will be deflected down toward the true transition state that leads to the cis product. We conclude that the transition state that directly leads to the trans product does not exist in the H_2 oxidative addition. This is consistent with the correlation diagram discussed in the preceding section that the trans addition of H_2 is symmetry forbidden.

There occurs a question why only the trans product is detected by experiment. Before discussing this problem, we must consider the change of relative stability of cis and trans products caused by a steric repulsion between phosphine ligands. We note that all the compounds used in the experiments have bulky phosphines such as PPh_3 and $P(t\text{-}Bu)_3$ rather than PH_3 in our model system. We will estimate the steric repulsion effect by calculating the RHF interaction energy between two isopropylphosphines, $PH_2(i\text{-}Pr)$. As shown in Figure 5, two phosphorus atoms of isopropylphosphines are placed at a distance of 2.194 Å, the PtP bond length in $Pt(PH_3)_2$, from the empty origin Z and the PZP angle is changed between 120° and 180°. In the calculation the structure of $PH_2(i\text{-}Pr)$ is fixed at an optimized geometry of a free state within C_s symmetry. The calculated interaction energy ΔE and the shortest isopropyl H–H distance R_{HH} are shown in Figure 5. One finds that at the PZP angle of about 140° R_{HH} is reduced to the sum of the hydrogen van der Waals radii, 2.4 Å, and the steric repulsion becomes very serious. In real Pt diphosphine compounds bulky phosphines will readjust their geometry to reduce the steric repulsion between them. Therefore the interligand angle where the steric repulsion becomes severe should be smaller than that obtained from the present model calculation. From these results we deduce that the steric repulsion between bulky phosphines is not serious at the transition state, where the PPtP angle is 148°. However, in *cis*-$Pt(H)_2(PR_3)_2$ the repulsion is expected to be very large, making this complex much less stable than the corresponding trans complex. We note that Noell and Hay estimated the steric repulsion to be 7 kcal/mol at the PPtP interligand angle of 100°, by using trimethylphosphine ligands.

On the basis of these discussions, one may imagine potential energy profiles shown in Scheme II involving only one early and cis-leading transition state. In the scheme the x direction stands for an in-plane H_2 approach and the y direction a perpendicular approach to the PPtP plane, dots specify the reactant and products, T means the transition state, and X represents the unaccessible "transition state". In Scheme IIa where the interligand steric repulsion is negligible, a deep valley path efficiently leads the system to the cis product. In Scheme IIb where bulky phosphines are used, the system still goes through the same early transition state where the steric repulsion is not yet serious, and, as it approaches the product, the steric repulsion has a good chance to push the system away from the cis product and lead to the less hindered trans product. There are three possible mechanisms of trans product formation: (1) the four-coordinate mechanism as shown in Scheme IIb, (2) the three-coordinate mechanism in which one of the bulky phosphines is lost, so that the steric repulsion between them is released, and (3) the five-coordinate mechanism. Experimentally the oxidative addition of H_2 takes place in benzene, toluene, and *n*-hexane,[4,5] less coordinating solvents; and therefore the first two mechanisms are more plausible than the last. Although the present calculation does not show which of the first two actually takes place, it can be said that the steric repulsion between the bulky phosphines is one of the important keys of the reaction, and experimental studies with less bulky phosphines would shed more light in elucidating the detailed mechanism.

Table XI. Analysis of Kinetic Deuterium Isotope Effect at 250 K for the Reductive Elimination *cis*-$Pt(X)(CH_3)(PH_3)_2 \rightarrow CH_3X + Pt(PH_3)_2$ (X = H and D)[a]

	reactant		transitn state		Π_i
mode (sym)	ν,[b] cm^{-1}	R_i	ν,[b] cm^{-1}	R_i^*	$R_i^* R_i^{-1}$
XPtC in-plane bending (A′)	1150	0.55	1030i	1.27	
	680	0.98			1.80
			1090	0.82	
			1430	0.94	
XPt stretching (A′)	2160	0.23	2170	0.34	1.16
			1630	0.79	
XPtC out-of-plane bending (A″)	780	0.85	1080	0.80	
	490	0.91	430	0.93	0.94
			580	0.99	
			620	0.99	
total[c]		0.096		0.19	1.97

[a] Only factors contributing significantly to the isotope effect are listed. [b] The frequencies are those in hydride compounds $Pt(H)(CH_3)(PH_3)_2$. [c] Total product of contributions of all the modes where for PH_3 rotations around PtP bonds, which have near-zero frequencies, their R_i and R_i^* are assumed to be 1.

(B) Transition State and Kinetic Isotope Effect in the Reductive Elimination of CH_4 from *cis*-$Pt(H)(CH_3)(PH_3)_2$. The reductive-elimination reaction of CH_4 from $Pt(H)(CH_3)(PPh_3)_2$ has been found by Abis, Sen, and Halpern.[8] The reaction rate was unaffected by the presence of excess triphenylphosphine, suggesting strongly that the elimination proceeds through a four-coordinate transition state. A large deuterium kinetic isotope ratio of 3.3 was observed for the decomposition reaction of $Pt(D)(CH_3)(PH_3)_2$.

We have searched the transition state for the reaction $CH_4 + Pt(PH_3)_2 \rightarrow Pt(H)(CH_3)(PH_3)_2$, the oxidative addition of CH_4 to $Pt(PH_3)_2$, and the reductive elimination of CH_4 from *cis*-$Pt(H)(CH_3)(PH_3)_2$, the arrows shown in Figure 3 indicate the reaction coordinate vectors. Normal-mode frequencies are given in Table IV, where the imaginary frequency of 1030i cm^{-1} corresponds to the reaction coordinate.

The conformation of the transition state has the following features: (1) the PPtP angle of 119° is much smaller than that of 148° at the transition state for the H_2 oxidative addition, (2) the PtC distance of 2.27 Å is 14% longer than that of 2.00 Å in the reactant *cis*-$Pt(H)(CH_3)(PH_3)_2$, (3) the CH distance of 1.35 Å is 25% longer than that of 1.08 Å in the product CH_4, and (4) the PtH distance of 1.59 Å is only a 4% increase from that of 1.52 Å in *cis*-$Pt(H)(CH_3)(PH_3)_2$. The first three features indicate that the transition state is located at a midpoint on the potential energy hypersurface between *cis*-$Pt(H)(CH_3)(PH_3)_2$ and $Pt(PH_3)_2+CH_4$. This is in contrast with the case of H_2, where the transition state is located near $Pt(PH_3)_2 + H_2$. The last feature shows that, though the reaction is concerted, two bonds do not break simultaneously in the elimination reaction. The weaker C–Pt bond is substantially broken before the H–Pt bond is replaced by a new C–H bond. In the reverse oxidative-addition reaction, of course, the H–Pt bond is formed in an early stage of reaction.

Interestingly the reaction coordinate at the transition state in Figure 3 has characteristics of HPtC bending rather than PtH stretching. It is important, therefore, to find out whether this transition state is consistent with the large observed kinetic deuterium isotope ratio of 3.3.[8] We have calculated and analyzed the isotope effect by using the Bigeleisen equation[51] and have given the results in Table XI. The calculated ratio of 2.0 is in reasonable agreement with the experimental value. The largest contribution to the calculated ratio is mainly due to 1.80 of the HPtC bending mode, as expected from the transition-state reaction coordinate.

We have also calculated the deuterium kinetic isotope ratio in the reverse reaction, the oxidative addition, of CH_3D and CD_4 to $Pt(PH_3)_2$ and obtained values of 6.7 (250 K) and 5.0 (300 K) for CH_3D and 17.0 (250 K) and 12.0 (300 K) for CD_4. The CH_4

Table XII. Energy Decomposition Analysis[a] of the Activation Energy of the Oxidative Addition of H_2 to $Pt(PH_3)_2$ (in kcal/mol)

deformation	
$Pt(PH_3)_2$	3.1
H_2	0.3
sum	3.4
interaction	
ES + EX	16.9
BCTPLX	−7.2
FCTPLX	−10.7
residue	2.8
sum	1.8
total	5.2

[a] With the larger basis set.

addition reaction has not been observed; however, the calculated isotope ratio will be useful to the future kinetic study of CH bond addition reactions such as orthometalations.[52]

In order to discuss the reaction mechanism in detail, the effect of the steric repulsion between bulky phosphines has to be considered as they are usually used in experiments. As discussed in the previous section, the repulsion will be serious in the cis compound, where the PPtP angle is about 120°. This destabilization would make the oxidative addition endothermic, which explains why the reaction has not been observed, and the reverse reductive elimination becomes exothermic. Accompanied with this change, the position of the transition state on the reaction coordinate should move further toward the cis compound, which is in contrast with the less affected transition state in the H_2 reaction. This implies that the possibility of unimolecular isomerization of cis hydride methyl compound $Pt(H)(CH_3)(PR_3)_2$ is small, because the proximity of this transition state would lead to decomposition. The change of location of the transition state will also modify the reaction coordinate vector. However, the HPtP bending mode will remain to be an important component of the reaction coordinate, since the PtH distance at the transition state is almost the same as that in the cis compound. Therefore, a large isotope due to the HPtP bending mode is expected to remain.

(C) Important Factors for Reaction. Two possible ways of a bond activation by metal compounds are known: a forward electron transfer from a bonding orbital of a breaking bond into vacant metal orbitals[53] and a backward electron transfer from occupied metal d orbitals into an antibonding orbital.[54,55] Dedieu et al.[20] and Lauher et al.[22] have pointed out from theoretical studies that the backward electron transfer is important in the stabilization of the transition state of the H_2 addition reaction. In order to examine the charge redistribution, we have carried out Mulliken population analysis at the transition states of $Pt(PH_3)_2 + HX$ (X = H and CH_3), as given in columns 8 and 9 of Table I. One finds at the H_2 addition transition state that the population 1.82 of Pt d_{yz} is smaller than 1.88 of the reactant and that the population 0.17 of Pt p_y is larger than 0.02 of the reactant. Though columns 2 and 5 of Table I show that just a bend of PH_3 ligands causes similar changes in the population, their magnitude is much smaller than the change found at the H_2 addition transition state. The above changes suggest both the backward electron transfer from the Pt d_{yz} orbital to H_2 σ^* and the forward transfer from H_2 σ to Pt p_y are important at the transition state. This will soon be confirmed by the energy analysis.

In order to investigate further the nature of electronic interaction, we have carried out the energy decomposition analysis (EDA)[56] at the transition state of the H_2 addition reaction. In the EDA, the RHF interaction energy is decomposed into the deformation energy of fragments from their equilibrium geometries and the electronic interaction energy among fragments. The latter energy is further decomposed into the sum of electrostatic and exchange interaction (ES + EX) between fragments, the forward and the backward charge-transfer interaction, FCTPLX and BCTPLX, respectively, and the residual interactions. In the present analysis $Pt(H)_2(PH_3)_2$ is divided into $Pt(PH_3)_2$ and H_2 fragments and the interaction between them is investigated. Results are given in Table XII, where a negative number means

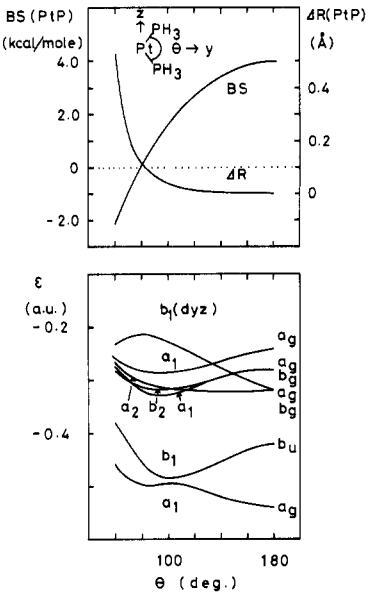

Figure 6. PtP bond strength (BS) and orbital energy ϵ of higher occupied orbitals in $Pt(PH_3)_2$ as functions of the PtP angle. The BS is the energy difference between $Pt(PH_3)_2$ and $Pt(PH_3)_2 + PH_3$ at each PPtP angle. The MO symmetry in the lower figure is the same as that in Figure 1. The smaller basis set.

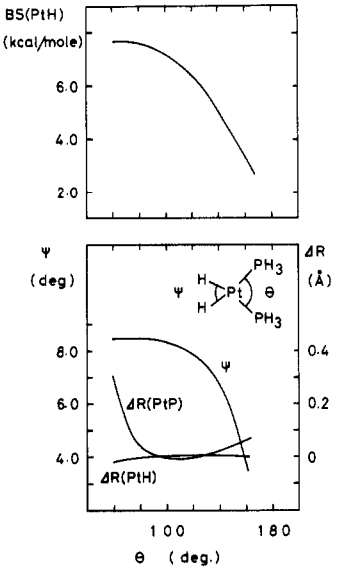

Figure 7. PtH bond strength (BS), PtH and PtP bond distances, and HPtH bond angles, ψ in *cis*-$Pt(H)_2(PH_3)_2$ as a function of the PPtP angle, θ. The BS is a half of the energy difference between $Pt(H)_2(PH_3)_2$ and $Pt(PH_3)_2 + H + H$. The bond distances are relative to those at the angle θ of 100°. The smaller basis set.

a stabilization.

In the H_2 addition reaction the energy required to deform two fragments from the equilibrium geometry to the geometry taken at the transition state is only 3.4 kcal/mol, typical of an "early transition state". The electronic interaction energy is 1.8 kcal/mol repulsive, where the electrostatic and exchange destabilization of 17 kcal/mol is nearly compensated by the forward charge-transfer (FCTPLX) stabilization of 11 kcal/mol as well as the backward charge-transfer (BCTPLX) stabilization of 7 kcal/mol. The "oxidation" of the metal will occur at some later stage of the reaction when the HH bond is actually broken.

The large backward charge-transfer interaction, BCTPLX, is consistent with the decreased total gross population in metal d and p_z orbitals. The large forward electron-transfer, FCTPLX, stabilization is reflected in the increased d_{y^2} and p_y population at the transition state. This FCTPLX interaction indicates that the

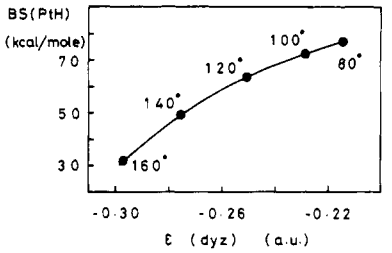

Figure 8. The relation between the bond strength of PtH in *cis*-Pt-$(H)_2(PH_3)_2$ and the d_{yz} orbital energy in $Pt(PH_3)_2$. The numbers in the figure are the value of the PPtP angle. The smaller basis set.

metal is in a sense "reduced" as well as "oxidized" at an early stage of the reaction.

In order to control the reactivity of two-coordinate Pt(0) and Pd(0) diphosphine compounds, Otsuka et al. suggested to consider the interligand angle as well as the steric size and basicity of phosphine ligands.[4,5,17] We have calculated the PtP bond strength and orbital levels in $Pt(PH_3)_2$ and PtH bond strength in *cis*-Pt-$(H)_2(PH_3)_2$ as functions of the PPtP interligand angle and show the results in Figures 6 and 7, respectively.

In the two-coordinate $Pt(PH_3)_2$ the PtP bond strength is positive in the range of the PPtP angles from about 80° to 180° (Figure 6), which suggests that Pt-chelating phosphine complexes can exist at these PPtP angles. At PPtP angles less than 80° one of the phosphines will probably dissociate. The change of the PtP bond strength is estimated to be about 10 kcal/mol for a decrease in the PPtP angle of 10° in the range between 100° and 140°. Among the higher occupied MO's only a b_1 MO consisting mainly of the Pt d_{yz} orbital is destabilized as the PPtP angle decreases. Electrons in this MO transfer to the reactant such as H_2 in the oxidative addition. Therefore, a chelating phosphine having a small PPtP angle effectively raises the reactivity of Pt electrons.

The dependence of the PtH bond strength and three geometrical parameters, PtH and PtP distances and the HPtH angle, on the PPtP interligand angle in *cis*-$Pt(H)_2(PH_3)_2$ is shown in Figure 7. For a decrease of the PPtP angle by 10°, the PtH bond strength increases by about 10 kcal/mol, a dependence opposite to that of the PtP bond strength. We note that in the possible range of θ, the change in the PtH and PtP bond distance is small. Relationships among the PtH bond strength, the d_{yz} orbital energy, and the PPtP angle are depicted in Figure 8. The change of the PtH bond strength in *cis*-$Pt(H)_2(PH_3)_2$ correlates very well with the destabilization of the d_{yz} orbital.

The oxidative addition of methane to transition-metal compounds has been a challenging problem for experimentalists. Recently Graham and Bergman have independently succeeded in carrying out the reaction by using iridium compounds.[57,58] The presumed reaction intermediates CpIrX (X = CO, PMe_3) are structurally unsaturated and have open-shell electrons (**a**) or a vacant 5d orbital (**b**). They are probably highly reactive, as a

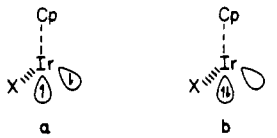

a b

vacant d orbital has been found to strongly activate a CH bond and makes the activation energy small for bond cleavage.[60] Although Pt diphosphine does not have a vacant d orbital, according to the above semiquantitative analysis there may be a possibility of CH_4 oxidative addition to Pt with a chelating phosphine such as $Pt[R_2P(CH_2)_3PR_2]$ (R = *t*-Bu) where the PPtP angle has been observed to be 102.6°,[5] although the dimerization such as observed by Yoshida et al.[5] has to be prevented in the first place.

Summary

Potential energy hypersurfaces of the reactions $H_2 + Pt(PH_3)_2 \rightarrow Pt(H)_2(PH_3)_2$ and $CH_4 + Pt(PH_3)_2 \rightarrow Pt(H)(CH_3)(PH_3)_2$ are investigated theoretically by fully optimizing the transition state as well as the equilibrium geometries. These two hypersurfaces show the following contrasts. The H_2 addition reaction is exothermic, while the corresponding CH_4 addition reaction is almost thermoneutral. The transition state of the former reaction is in an early stage with the PPtP angle of 148°, whereas that of the latter is at the midpoint with the angle of 119°. The activation barrier is only 8 kcal/mol in the former, while it is 28 kcal/mol in the latter. The reaction coordinate vectors consist mainly of the H_2 translational mode in the former and of the HPtP bending mode in the latter. The large hydrogen isotope effect observed for the CH_4 reductive elimination is consistent with the calculated transition state.

These differences in the potential energy hypersurfaces can be explained by the differences between the PtH and PtC bond strengths that are estimated to be 61–70 and 34–41 kcal/mol, respectively. The larger PtH bond strength results in a larger exothermicity, an earlier transition state, and hence a lower activation barrier.

The effect of the steric repulsion between bulky phosphines is expected to be different between H_2 and CH_4. In the H_2 addition reaction the effect would be negligible at the cis transition state but destabilizes the cis product. Therefore the system would easily go through the cis transition state and then deviate from the sterically undesirable cis path to reach the less destabilized trans product. In the CH_4 addition reaction the effect would be large even at the transition state, making the reaction all the more difficult.

The decrease of PPtP interligand angle activates efficiently and selectively one of the metal d orbitals. The activated energy is calculated to be about 10 kcal/mol per 10° change in the PPtP angle in the range from 100° to 140°.

Acknowledgment. We are grateful to Professors Sei Ohtsuka and Akio Yamamoto for stimulating suggestions and discussions. All the calculations were carried out by a program IMSPACK at the Computer Center of Institute for Molecular Science. IMSPACK includes a program for electronic integrals with ECP approximation coded by Dr. L. R. Kahn and a direct-CI program taken from ALCHEMY.

Registry No. *cis*-$Pt(H)(CH_3)(PH_3)_2$, 79232-17-0; *trans*-$Pt(H)(CH_3)(PH_3)_2$, 92541-64-5; *cis*-$Pt(H)_2(PH_3)_2$, 76832-29-6; *trans*-$Pt(H)_2(PH_3)_2$, 76830-84-7; $Pt(PH_3)_2$, 76830-85-8; CH_4, 74-82-8; H_2, 1333-74-0; D_2, 7782-39-0.

(60) (a) Dawoodi, Z.; Green, M. L. H.; Mtetwa, V. S. B.; Prout, K. *J. Chem. Soc., Chem. Commun.* **1982**, 802. (b) Koga, N.; Obara, S.; Morokuma, K. *J. Am. Chem. Soc.* **1984**, *106*, 4625. (c) Obara, S.; Koga, N.; Morokuma, K. *J. Organomet. Chem.* **1984**, *270*, C33.